Stem Cells, 2025, **43**, sxaf012
https://doi.org/10.1093/stmcls/sxaf012
Advance access publication 20 March 2025
Original Research

Nephron progenitor fate is modulated by angiotensin type 1 receptor signaling in human kidney organoids

Hyunjae Chung[1,‡], Waleed Rahmani[1,‡], Sarthak Sinha[2], Aysa Imanzadeh[1], Alexander Pun[2], Rohit Arora[2], Arzina Jaffer[2], Jeff Biernaskie[2,3,4], Justin Chun[*,1]

[1]Department of Medicine, Snyder Institute for Chronic Diseases, Cumming School of Medicine, University of Calgary, Calgary, AB, Canada T2N 4N1,
[2]Department of Comparative Biology and Experimental Medicine, Faculty of Veterinary Medicine, University of Calgary, Calgary, AB, Canada T2N 4N1,
[3]Hotchkiss Brain Institute, University of Calgary, Calgary, AB, Canada T2N 4N1,
[4]Alberta Children's Hospital Research Institute, University of Calgary, Calgary, AB, Canada T2N 4N1

[*]Corresponding author: Justin Chun, University of Calgary, Cumming School of Medicine, Health Research Innovation Centre 4A12, 3280 Hospital Drive NW, Calgary, AB, Canada T2N 4Z6 (chuj@ucalgary.ca).
[‡]These authors contributed equally.

Abstract

The renin-angiotensin system (RAS) is essential for normal kidney development. Dysregulation of the RAS during embryogenesis can result in kidney abnormalities. To explore how angiotensin type 1 receptor (AT_1R) signaling modulates nephron progenitor (NP) fate specification, we used induced pluripotent stem cell (iPSC) derived human kidney organoids treated with angiotensin II (Ang II) or the AT_1R blocker losartan during differentiation. Ang II promoted NP proliferation and differentiation preferentially toward a podocyte fate, depleted the podocyte precursor population, and accelerated glomerular maturation. By contrast, losartan expanded the podocyte precursor population, delayed podocyte differentiation, and regressed the transcriptional signature to a more immature fetal state. Overall, using various *in silico* approaches with validation by RNAscope, we identified a role for AT_1R signaling in regulating NP fate during nephrogenesis in kidney organoids. Our work supports the use of RAS modulators to improve organoid maturation and suggests that RAS may be a determinant of nephron endowment *in vivo*.

Key words: angiotensin II; kidney organoids; losartan; nephrogenesis; single-cell RNA sequencing.

Received: 10 June 2024; Accepted: 3 March 2025.

Graphical Abstract

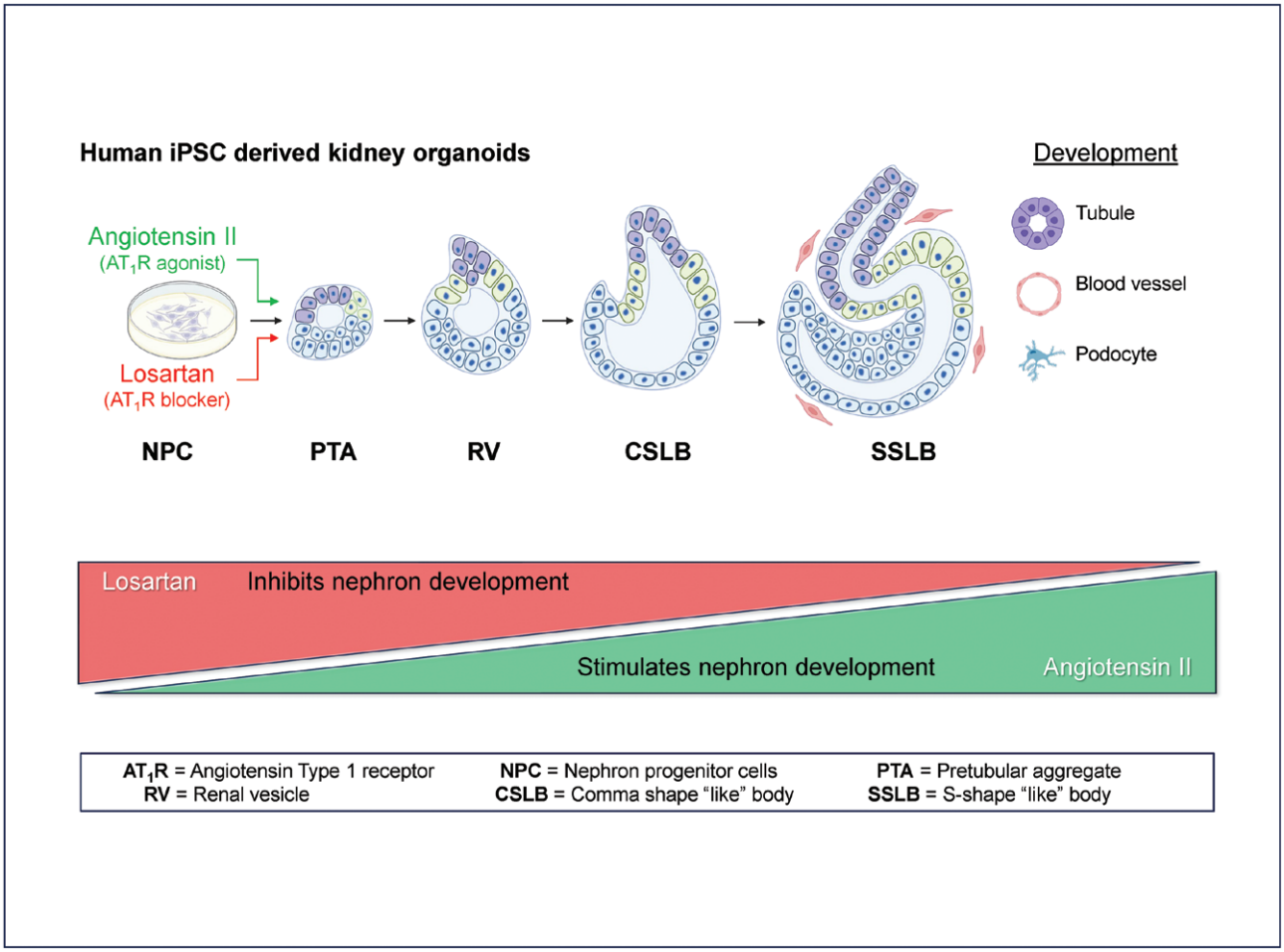

Significance statement

Kidney development is tightly regulated by the renin-angiotensin system. In this study, we use kidney organoids to demonstrate that angiotensin II can improve *in vitro* nephrogenesis and organoid maturation. Angiotensin type 1 receptor modulation influenced transcriptional and lineage behavior of nephron progenitors, podocyte precursors, endothelial cells, and distal tubular cells. Angiotensin II accelerated nephron progenitor differentiation toward maturity while losartan stalled progenitor differentiation and decelerated nephrogenesis. Overall, we provide evidence supporting the use of renin-angiotensin system modulators to enhance organoid maturation.

Introduction

Human kidney development is complete by 35-36 weeks of gestation when 250 000 to 2 million nephrons are established.[1] *SIX2*+ nephron progenitor (NP) cells are responsible for differentiating into podocytes, parietal epithelial cells (PECs), proximal tubule cells (PTC), loop of Henle (LoH), and distal tubule cells (DTC).[2–4] To ensure optimal nephron endowment, NP cells must maintain multipotency throughout gestation by balancing self-renewal and differentiation. *SIX1/2*+ along with *SALL1* and *EYA1* are transcription factors critical for maintaining the undifferentiated state, while *WNT*, *BMP*, *FGF*, and *NOTCH* signaling promote differentiation via mesenchymal-to-epithelial transition (MET).[5–12] The spatial segregation within the nephrogenic niche supports this balance, with uncommitted NP cells located near the ureteric tip and committed cells transitioning toward the tip of stalk junction. Low-level WNT signaling (*WNT9B*) near the ureteric tip preserves the undifferentiated state, while BMP signals inhibit premature differentiation. WNT4 is an auto-inductive signal that triggers and propagates nephron epithelialization after primary induction by WNT9B from the ureteric epithelium.[12-14] Additionally, stochastic migration of NPC between these regions allows flexible exposure to niche signals, ensuring the preservation of the progenitor pool while enabling differentiation.[15] The gradual outcome is NP exhaustion and the cessation of nephrogenesis by birth.[16] The molecular determinants of NP exhaustion are not well understood.[17,18]

The renin-angiotensin aldosterone system (RAS) regulates kidney organogenesis by guiding vascular, tubular, glomerular, and medullary development potentially contributing to nephron endowment.[12,19] Most RAS genes are expressed early in human kidney development including angiotensinogen, angiotensin-converting enzyme (ACE), renin (REN), angiotensin type 1 (AT_1R), and type 2 (AT_2R) receptors.[19,20] Inherited mutations can cause tubular dysgenesis, oligohydramnios, and perinatal death.[21,22] Indeed, inhibitors of ACE and the AT_1R

are contraindicated in pregnancy, particularly in late gestation, due to their fetotoxicity.[23,24] It is unclear whether RAS regulates NP fate during nephrogenesis. Interestingly, deletion of the prorenin receptor (PRR) in *Six2*$^+$ NP cells reduced murine nephron endowment and promoted podocyte foot process effacement with proteinuric kidney disease. Depleted NP cells reduced their proliferative capacity and diminished responsiveness to WNT signaling.[25] A lineage-specific role for RAS in NP cells during human nephrogenesis has not been well studied.

Induced pluripotent stem cell (iPSC) derived kidney organoids are valuable *in vitro* models to study kidney development and disease.[26-28] We sought to understand the role of AT_1R signaling in NP fate specification using angiotensin II (Ang II) and the angiotensin receptor blocker (ARB) losartan. We show that *SIX2*$^+$ podocyte precursor cells are exquisitely sensitive to AT_1R signaling. They preferentially differentiate toward a podocyte fate under Ang II showing enhanced phenotypic maturation. With losartan, the precursor population expanded at the expense of podocyte differentiation. Our study establishes a lineage-specific role for AT_1R in human kidney nephrogenesis and suggests that RAS signaling can be leveraged to fine-tune organoid development.

Results

Human kidney organoids develop a transcriptionally responsive renin-angiotensin system

Kidney organoids were generated similarly to a previously described protocol by Takasato et al and adapted by our group (Figure 1A-1C).[29-31] On day 28, unsupervised clustering of our scRNA-seq data revealed 21 distinct cell clusters (C0-20) identified by their expression of conserved genes described in prior scRNA-seq datasets[32-34] (Figure 1D and Supplementary Table S1). Podocyte subclusters (C0-C3) were analyzed for transcriptional signatures based on the scRNA-sequencing data from human fetal kidneys evaluating the differentiation of functional podocytes from progenitors.[34] In our kidney organoids, C2 expressed gene signatures consistent with NP cells, C1 early podocyte markers, and C0 late podocyte markers (Figure 1E). C3 had low expression of early podocyte markers and low transcripts suggesting either a distinctive podocyte precursor population or an artifact of low-quality/dying cells (data not shown). C0 cells were mostly enriched for *TCF21*, *MME*, *NPHS2, PODXL,* and *PLA2R1*, suggesting mature podocytes (Figure 1D and E). C1 cells were enriched for *ITIH5*, *CTGF*, *TSPAN8,* and *MAFB* but co-expressed early podocyte genes (*PAX8*, *OLFM3*, *SLC16A1*), indicative of a less mature podocytes state compared to C0 (Figure 1D and E). The podocyte maturation program initiates as early podocyte signature genes are transiently upregulated while NP signature genes are deactivated in NP cells.[34] C2 cells were enriched for early podocyte genes (*LYPD1*, *OLFM3, DAPL1, PAX8)* coincided with NP genes (*SIX1*, *SIX2, EYA1*), suggesting podocyte precursors (Figure 1D and E). *SIX2*$^+$ cells were detected in the peritubular and periglomerular space (Figure 1A and B). C3 cells were enriched for *AIF1*, *DAPL1*, *VAMP8, ANXA1* with minimal NP signature genes subclustered separately from C1 (Figure 1D and E). C4 cells were enriched for *PAX8, CLDN1,* and *CAV2* transcripts suggesting an early parietal epithelial cell (PEC) phenotype. There were two proximal tubular cell (PTC) clusters (C5,6), three distal tubular cell (DTC) clusters (C7-9), one endothelial cluster (C10), and three stromal clusters (C11-13). C11 resembled mesangial-like cells enriched for *REN, GATA3,* and *MGP* (Figure 1D). Compared to previous reports, the percentage of stromal cells and off-target cells is similar however our differentiation protocol generated more glomerular epithelial cells (30.1%) and fewer tubular cells (15.8%) which was not surprising as the variability between kidney organoids from different iPSC lines and experimental batches has been well documented.[35,36] On day 28, mRNA transcripts of critical RAS genes were detected in the expected cell clusters (Figure 1F). *CTSB* (cathepsin B) and *ATP6AP2* (pro-renin receptor) were expressed in nearly all cells. *AGT*, *ACE1,* and *ACE2* transcripts were predominantly in PTC. *AGTR1*, *AGTR2*, and *REN* transcripts were restricted to stromal cells, particularly mesangial cells (C11). When we re-clustered the stromal cells alone, *REN* expression was restricted to subcluster S3 (Supplementary Figure S1A and B). Signature genes for fetal human renin cells were also enriched in subcluster S3 (*REN*, *MEF2C*) and neighboring subcluster S1 (*MEF2C*, *ACTA2*, *MYH11*, and *TAGLN*) (Supplementary Figure S1B) suggesting that organoids developed renin-expressing cells transcriptionally similar to fetal juxtaglomerular cells.[34,37] Overall, these findings demonstrate that our kidney organoids developed key cell types including podocyte precursors, podocytes, and renin-producing cells, possessing RAS network features of the developing human kidney.

AT_1R signaling modulates the transcriptional activity of podocyte, endothelial, and distal tubule clusters

A previous study did not observe gene expression changes when day 12 organoids were chronically treated with RAS modulators.[38] To avoid post-transcriptional confounders, we limited our analysis to day 28 organoids treated for only 24 hours. Globally, Ang II and losartan upregulated gene expression more than they downregulated gene expression (Figure 2A). C2 population were the most transcriptionally activated cells (Figure 2A, Supplementary Figure S2A), followed by endothelial cells (C10; Supplementary Figure S3A) and distal tubule cells (C8; Supplementary Figure S3B) by Ang II treatment. Losartan alone preferentially activated C3 population (Supplementary Figure S2B). Co-incubation of losartan with Ang II abrogated the transcriptional changes induced by Ang II alone (Figure 2A), suggesting that these transcriptional effects of Ang II are partially AT_1R-mediated and inhibited by losartan.

Next, we undertook a gene ontology (GO) enrichment analysis of gene sets for the podocyte precursors, endothelial cell, and distal tubular cell clusters processing genes in terms of their associated biological process (Supplementary Table S2) using threshold fold changes of >1.2-fold or <0.8-fold over control in response to Ang II or losartan. GO enrichment analysis in podocyte precursors (C2) revealed that Ang II upregulated pathways related to kidney epithelium development, podocyte differentiation, glomerular epithelial cell development, and nephron epithelium morphogenesis. Conversely, losartan downregulated pathways related to nephron development, glomerular epithelial cell development, podocyte development, and podocyte differentiation (Supplementary Figure S2A). Notably, the 108 genes commonly upregulated by Ang II and downregulated by losartan were enriched for pathways related to podocyte development,

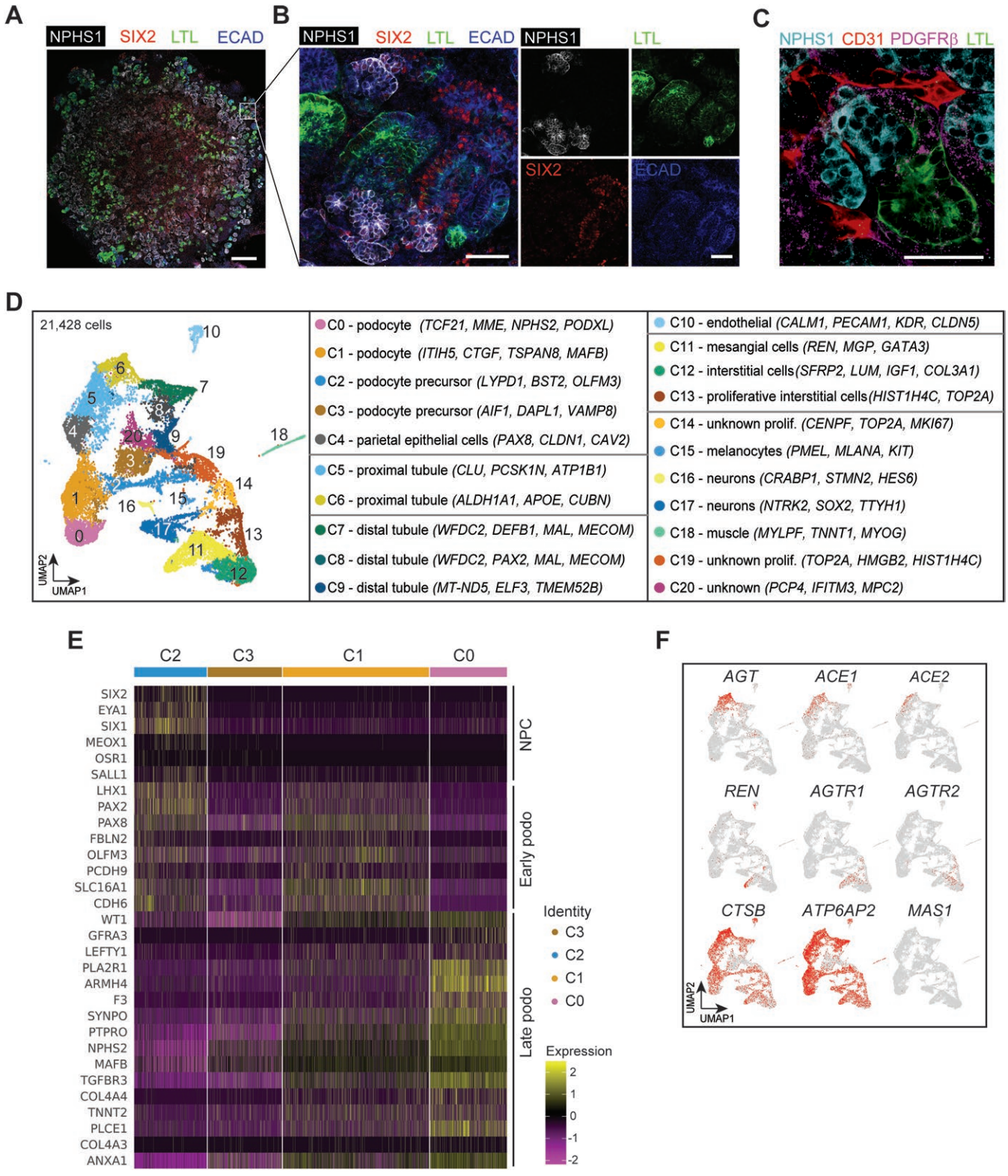

Figure 1. Human kidney organoids and RAS expression.. (A-C) Immunofluorescence staining of kidney organoids showing the major nephron structures generated including proximal tubules (LTL; Lotus tetragonolobus lectin), distal tubules (ECAD; E-cadherin), podocytes (NPHS1; nephrin), nephron progenitors (SIX2), stromal cells (PDGFR-β), and endothelial cells (CD31). Scale bars, 500 μ m for panel A and 50 μ m for panels B and C. (D) UMAP presentation showing 21 428 high-quality cells profiled from 4 kidney organoids at day 28 of Takasato protocol. 21 cell clusters were annotated by querying canonical marker genes. (E) Heatmaps showing the expression of selected signature genes for NP, early and late podocyte in C0-C3 clusters. (F) Feature plots showing the expression of RAS genes in kidney organoids.

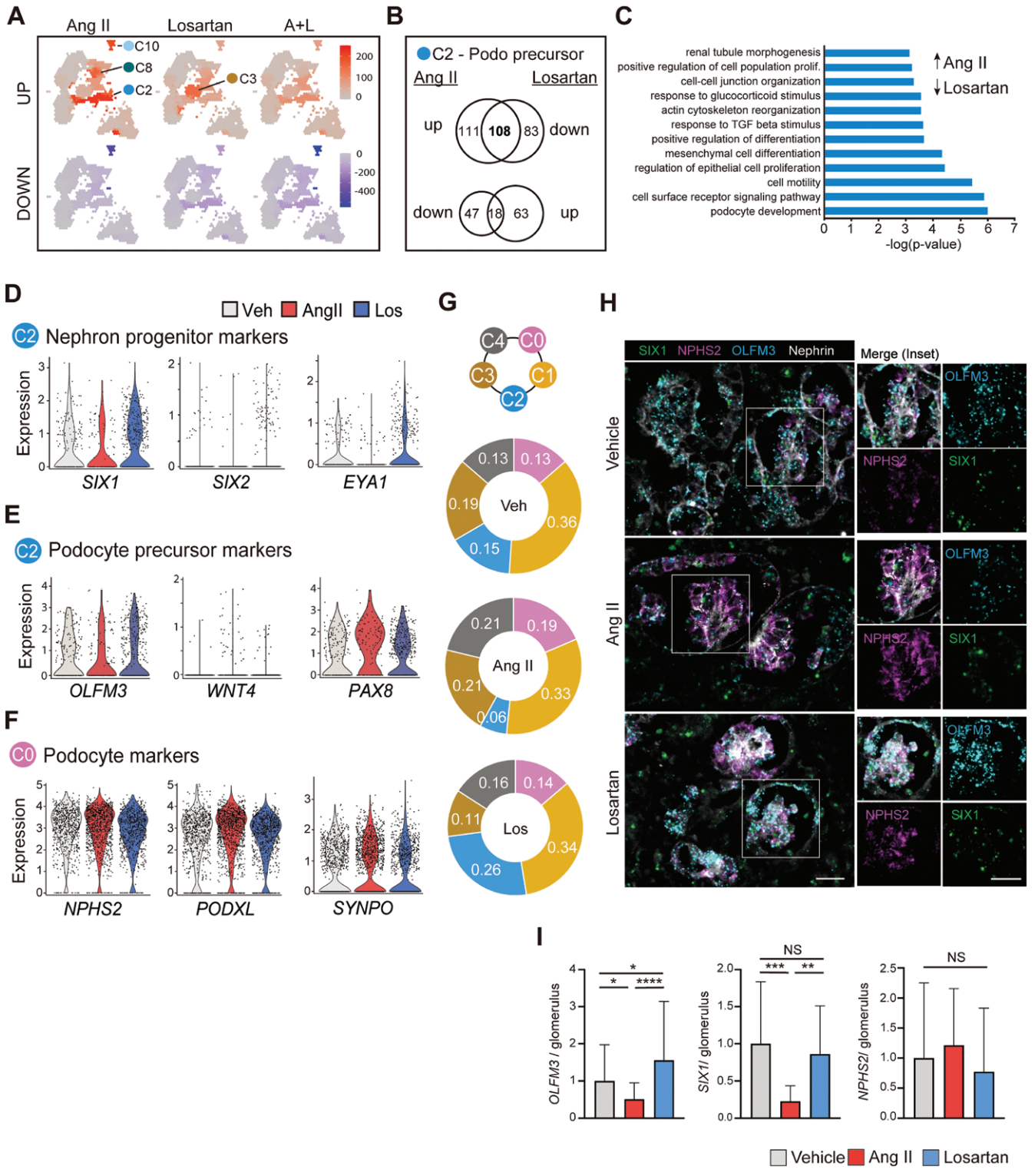

Figure 2. Podocyte precursor activation by Ang II in an AT_1R-dependent fashion. (A) UMAP presentation, excluding off-target cells, overlaid with log_2[fold change] of the most differentially expressed genes (DEGs) per cluster. (B) Venn diagrams of the DEGs in the podocyte precursor 1 cells (C2). (C) Gene ontology enrichment analysis of 108 differentially expressed genes upregulated by Ang II and downregulated by losartan in C2 cells. (D-F) Differential expression of genes indicative of nephron induction and podocyte precursor markers. (G) Pie charts depicting the relative quantity (%) of cells within clusters 0-4. (H-K) RNAscope images and quantitative analysis of *OLFM3, SIX1,* and *NPHS2* expression in kidney organoids treated with Ang II or losartan (n = 23-32 glomeruli, three biological replicates). Scale bar, 2 0 μ m. NS, not significant, Data are mean ± SD. *P < .05, **P < .01, ***pP < .001, ****P < .0001. One-way ANOVA with post-hoc Tukey's multiple comparisons.

epithelial cell proliferation, cell motility, and mesenchymal cell differentiation, suggesting a role for AT_1R in promoting podocyte differentiation (Figure 2C; FDR $P < .05$). C3 cells showed no enrichment for podocyte differentiation-related pathways, but losartan treatment upregulated pathways enriched for regulators of protein translation including protein folding, translational initiation, miRNA inhibition, and vesicle-mediated transport (Supplementary Figure S2B and Supplementary Table S2).

In endothelial cells (C10), Ang II upregulated pathways related to hypoxia, glomerular epithelial cell differentiation, comma-shaped body morphogenesis, distal tubule development, and cell proliferation involved in kidney development (Supplementary Figure S3A). Consistently, losartan downregulated pathways related to blood vessel morphogenesis, blood vessel development, and vascular development. Interestingly, Ang II downregulated pathways related to vascular permeability regulation, branching morphogenesis, and angiogenesis which may be more important for vasculogenesis and angiogenic remodeling that follow endothelial cell proliferation.

In distal tubule cells (C8), Ang II upregulated pathways related to tube development, renal system development, and nephric duct morphogenesis while losartan downregulated pathways related to tube morphogenesis and regulation of branching involved in ureteric-bud morphogenesis consistent with AT_1R-mediated signaling contributing to distal tubule maturation (Supplementary Figur eS3B). Interestingly, no significant effects of Ang II or losartan were observed in proximal tubule cells (C5) (Supplementary Figure S3C). Taken together, the pathways involved in the differentiation and maturation of podocytes, endothelial cells, and distal tubular cells are stimulated by Ang II and inhibited by losartan.

Given that C2 showed the highest transcriptional sensitivity and enrichment for pathways related to podocyte differentiation in our GO analysis, we sought to determine whether Ang II regulates podocyte differentiation. Further analysis of the C2 population revealed gene expression changes, where Ang II upregulated inducive markers including *WNT4* and *PAX8*, and downregulated NP progenitor markers including *SIX1* and *SIX2* (Figure 2D and E).[7,13,39] Ang II depleted the number of C2 cells by 43.2% and expanded the pool of mature podocytes (C0) and PECs (C4) (Figure 2G). On the other hand, losartan upregulated markers of the progenitor state including *SIX1*, *SIX2, and EYA1* in C2 cells (Figure 2D and G).[3,5,40] Further, losartan decreased the expression of *NPHS2*, *PODXL,* and *SYNPO* in the podocyte cluster (C0; Figure 2F), while upregulating *OLFM3* in C2 cells (Figure 2E). Our scRNA results suggest that Ang II promotes a shift from the C2 population to C0 for enhanced podocyte maturation, while losartan may drive pre-podocyte state.

To validate our scRNA seq data, we performed RNAscope on kidney organoids treated with vehicle, Ang II, and losartan for 24 hour. We anticipated that Ang II would promote the expression of podocyte markers (C0) by reducing the expression of NP genes (*SIX1, SIX2*) and podocyte precursor markers (*OLFM3*). Indeed, Ang II-treated organoids showed decreased expression of *SIX1* (1.00 vs 0.23, $P = .0005$) and *OLFM3* (1.0 vs 0.51, $P = .033$ in podocytes (Nephrin + glomeruli) compared to vehicle controls (Figure 2H and I). Losartan-treated organoids showed increased expression of *OLFM3* (1.00 vs 1.56, $P = .016$, Figure 2H and I), corroborating the scRNA sequencing results. *NPHS2* expression trended higher with Ang II and lower with losartan treatment, but the differences were not statistically significant (Figure 2I). Taken together, our scRNA-seq analysis and RNAscope experiments reveal that Ang II promoted podocyte maturation programs and expanded the pool of mature podocytes in an AT_1R-mediated fashion. By contrast, losartan appears to favor the progenitor state by inhibiting the mesenchymal-to-epithelial transition during nephrogenesis.

Angiotensin II activates signaling between AT_1R^+ stromal cells and *SIX2*$^+$ podocyte precursors

Podocyte precursor clusters C2 and C3 were the most sensitive clusters to Ang II and losartan, respectively, yet *AGTR1* and *AGTR2* expression was predominantly in stromal cells (C11-13; Figure 3A) as described previously.[38] Does AT_1R modulate NP cells indirectly through AT_1R^+ stromal cells? Indeed, stromal cell signaling is important for nephron differentiation during development.[41] After Ang II treatment, mesangial-like stromal cells (C11) upregulated genes that regulate chemotaxis, MAP kinase activity, and cell migration (Supplementary Figure S3D). We evaluated paracrine signaling between stromal (C11-13) and glomerular epithelial cells (C0-4) using an approach whereby cluster-wise mean expression of literature-supported ligands and surface receptors present in the FANTOM5 database were calculated.[42] When a cognate ligand-receptor pair was expressed in at least 20% of cells and upregulated by 1.3-fold, an edge connecting the two cell clusters was calculated and plotted on a circos plot to denote a predicted signaling axis (Figure 3B and Supplementary Table S3). Ang II preferentially upregulated ligand-receptor pairs between stromal clusters (C11-13) and podocyte precursor (C2) through the Notch pathway (*DLK1*, *NOTCH1*, *NOTCH2*), collagens (*COL2A1*, *COL8A1*, *COL11A1*), integrins (*ITGA1*, *ITGA2*), and *MMP9* (Figure 3B). Indeed, ECM-mediated cell-cell contacts and Notch signaling are known determinants of progenitor lifespan and *SIX2* expression during development.[6,17] Therefore, our *in silico* analysis suggests that Ang II indirectly activates NP differentiation through cell-cell contacts with AT_1R^+ mesangial cells possibly via the ECM and Notch signaling. Immunostaining of kidney organoids treated with either Ang II or losartan did not have any obvious changes in AT_1R or SIX2 protein expression or distribution due to treatments (Fig. 3C). However, we did in fact observe AT_1R surface expression on stromal cells interlaced between NPHS1$^+$ cells that had low levels of SIX2 expression (Figure 3C). The SIX2-positive cells localizing to areas positive for AT_1R may be suggestive of a transition of residual nephron progenitors as they are not capable of self-renewal or ongoing nephrogenesis.[43]

AT_1R activation directs NP differentiation towards a podocyte fate

Next, we examined the effect of AT_1R signaling on progenitor fate decisions using scVelo, a likelihood-based dynamic model that evaluates the rate of gene expression change for individual genes (RNA velocity) based on the ratio of its spliced and unspliced mRNA.[44] A new UMAP comprised of C0-C9 clusters was generated and overlaid with vector fields and denoted as C′0-13 (Figure 4A-C). Two large clusters emerged representing the PTC (C′2 and C′6), DTC (C′5 and C′10) and podocyte lineages (Figure 4A). NP cells (*CITED1, SIX2)* resided within 2 clusters (C′11, C′13) positioned between the tubular and podocyte clusters (Figure 4A). Four clusters were

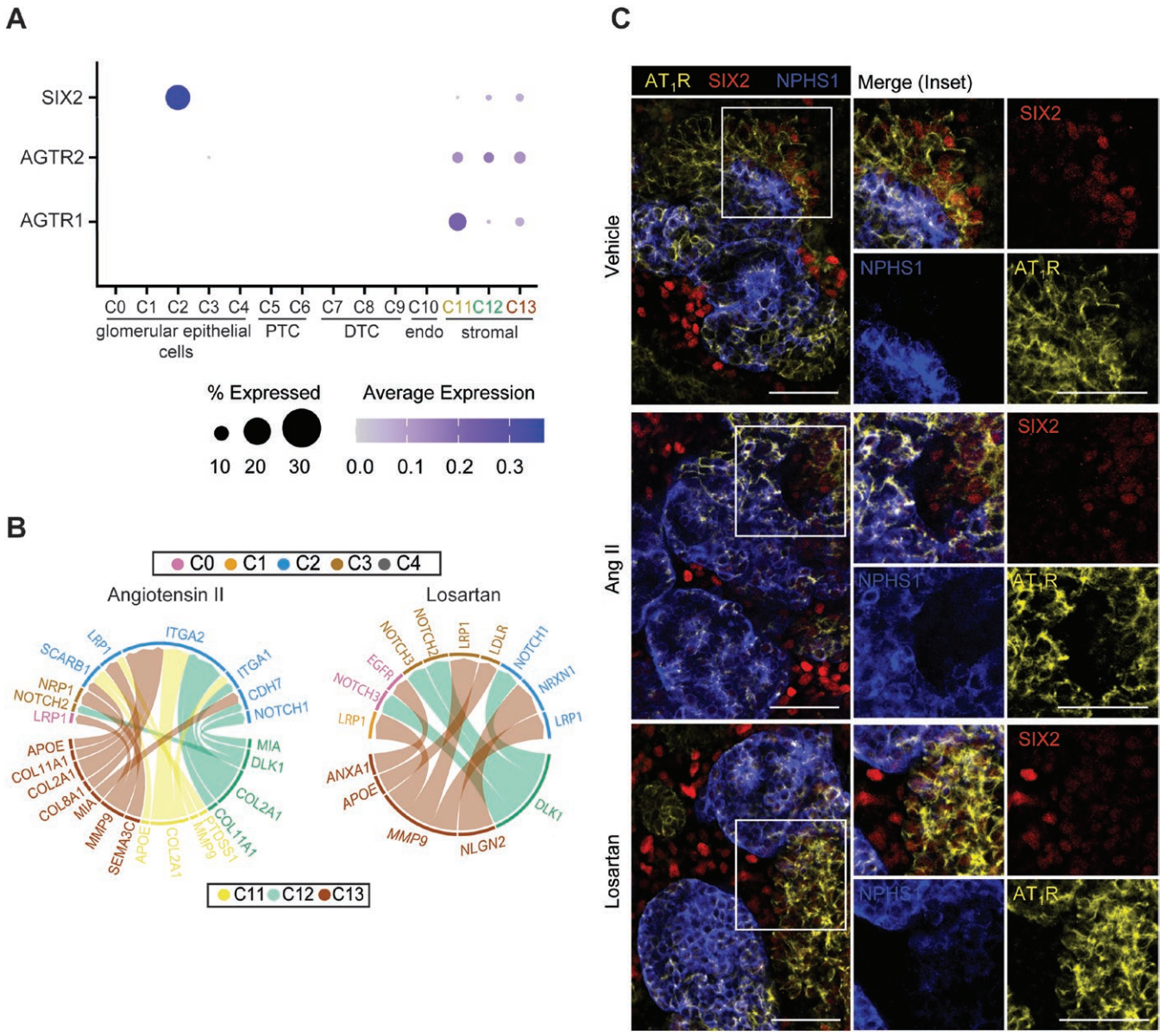

Figure 3. Ligand–receptor analysis between stromal cells and NP cells. (A) SIX2, *AGTR1,* and *AGTR2* mRNA expression across the major kidney cell clusters (C0-13). (B) Receptor-ligand analysis between stromal cells (C11-13) and podocyte lineage (C0-4) highlighting receptor-ligand connections upregulated by Ang II and losartan. (C) Day 25 organoids immunostained with AT_1R, NPHS1, and SIX2 representative of 3 biological replicates. Scale bar, 50 μm.

identified as terminal "end points": clusters C′1 (podocyte), C′2 (PTC), C′5, and C′10 (DTC). Podocyte precursors (*OLFM3, SLC16A1)*, early podocytes, and parietal epithelial cells (*CLDN1, CAV2*) were transitionary states between NP cells and podocytes. NP differentiation was biased towards the podocyte lineage in untreated organoids and tubular cells were primarily derived from cluster C′6 which may represent tubular precursor cells (Figure 4B).

AT_1R signaling preferentially altered the vector fields along the podocyte lineage (Figure 4D). Ang II accelerated state transition toward PEC (C′4) and podocyte fates (C′0,1,8) while depleting the NP (C′11,13) and podocyte precursor (C′7) clusters, consistent with the RNAscope data (Figure 2H and I). The most differentially spliced genes by Ang II were receptors associated with the integrity of podocyte foot processes (*CLIC5*),[45] genetic podocytopathies (*DLC1*)[46], and autoimmune podocytopathies (*PLA2R* and *THSD7A*) (Figure 4E). Using *Dynamo*,[47] a computational framework that allows for *in silico* gene perturbations to predict cell-fate transitions, we show that *in silico* upregulation of known gene drivers of the podocyte fate (*PTPRO, ROBO2,* and *TGFBR2*) generated vector fields resembling Ang II (compare Figure 4D and F). Contrastingly, losartan stalled podocyte differentiation at the NP state. The pool of NP and podocyte precursors increased at the expense of early (C′0,8) and mature (C′1) podocytes. Losartan dampened Ang II's effect on NP differentiation in co-treated organoids again suggesting this is an AT_1R-mediated effect. We did not observe significant alterations in the RNA velocity trajectories within the tubular lineage (see Discussion).

Next, we performed an unbiased feature selection of weeks 15 and 17 human fetal kidney transcriptomes using scPred

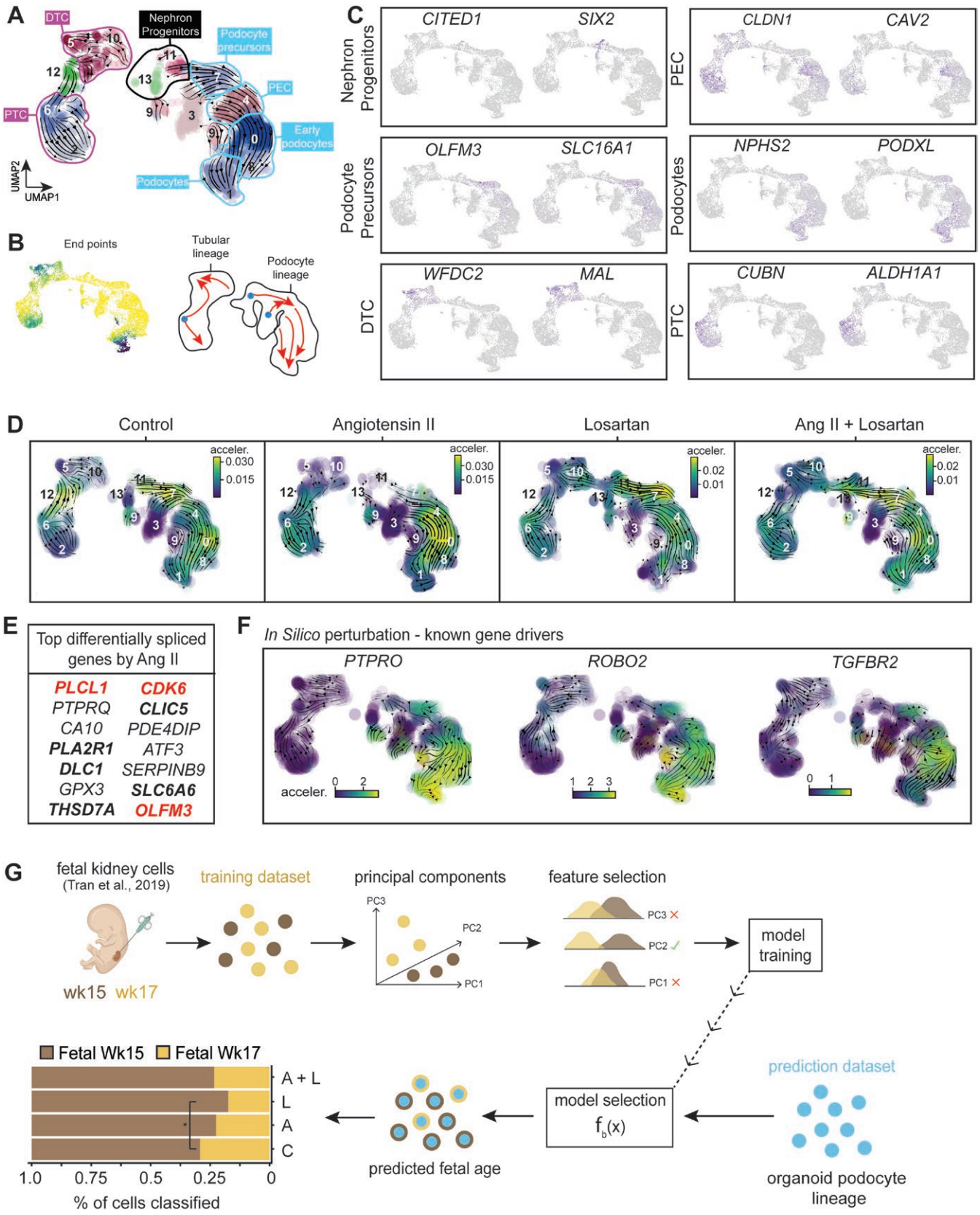

Figure 4. Nephron progenitor differentiation toward a podocyte fate with Ang II. (A-B) RNA velocities portrayed as stream-line plots on UMAP of nephron progenitors, PTC, DTC, podocyte precursors, PEC, and podocytes in control organoids. UMAP comprised of C0-C9 clusters was generated and overlaid with vector fields and denoted as C′0-13. (C) Inference of cell trajectories by end cell analysis. (D) Acceleration vector fields showing differential NP fate in control and treated organoids. (E) Top differentially spliced genes in NP cells and the podocyte lineage after Ang II treatment. (F) *In silico* perturbation of known gene drivers of podocyte fate (*PTPRO*, *ROBO2*, *TGFBR2*) using DYNAMO. (G) Schematic of scPred-based machine learning classifier trained to distinguish between human fetal weeks 15 and 17 and subsequently applied to cells from podocyte lineage including NPs.

and trained a prediction model to accurately discriminate between the two fetal ages (Figure 4G).[34,48] Most cells from the podocyte lineage, including NPs were classified as week 15. There was no significant difference in classification rates between control and Ang II organoids. However, losartan significantly increased classification rates for week 15 suggesting that AT_1R inhibition stalls transcriptional maturation of the podocyte lineage (0.73 vs 0.82; $P = .04$, chi-square test; Figure 4G). Taken together, our *in silico* analyses support transcriptional regulation of AT_1R signaling on NP behavior and differentiation through the podocyte lineage.

Nephron development is regulated by AT_1R signaling

We next sought to examine how AT_1R activity perturbs nephron development by examining changes to nephron morphology. Beginning at day 10, kidney organoids were treated for 5 days with vehicle, Ang II, or losartan in 2 separate iPSC lines (Figure 5 and Supplementary Figure S4). By day 16, compared to control, Ang II from CLi001-A organoids had larger glomeruli (31.3 vs 38.8 µm; Figure 5B and D) while losartan organoids had smaller glomeruli (31.3 vs 24.1 µm; $P < .001$, Figure 5B and D). Fewer NPHS1$^+$ synaptopodin$^+$ podocytes were Ki67$^+$ after Ang II treatment, indicating increased terminal differentiation (53.6 vs 26.0%; $P < .0001$; Figure 5C). Ki67$^+$ NPHS1$^+$ synaptopodin$^+$ cells were similar for vehicle and losartan treatment (53.6 vs 58.9%; $P = 0.34$) (Figure 5C). Similar to organoids derived from the CLi001-A line, glomeruli were larger following treatment with Ang II in the 1481 line (79.8 vs 109.3 µm; $P < .001$) with fewer NPHS1$^+$ Ki67$^+$ cells (80.6 vs 24.4%; $P < .001$, Supplementary Figure S4A-C). Losartan organoids had smaller glomeruli (79.8 vs 59.0 µm; $P < .001$; 1481) with comparable NPHS1$^+$ Ki67$^+$ cells to the control (80.6 vs 70.5%; $P = 0.5$, 1481, Supplementary Figure. S4A-C). The scRNA-seq data corroborated the inverse correlation between active replication (% in S phase) and podocyte maturity (*NPHS2* expression) (Supplementary Figure S4D).

The nascent nephron begins as a cluster of mesenchymal cells comprised of SIX2$^+$ NP cells called the pretubular aggregate (PTA). The PTA epithelializes to form a small cyst-like renal vesicle (RV) before differentiating and elongating into comma-shaped body (CSB), S-shaped body (SSB), capillary loop nephron (CLN), and finally an adult nephron.[4] As opposed to cellular hypertrophy or disorganized growth, we hypothesize that AT_1R modulated nascent nephron size by regulating procession through the stages of nephrogenesis (PTA-RV-CSB-SSB-CLN). We were able to identify PTAs, RVs, comma-shaped "like" bodies (CSLB) and S-shaped "like" bodies (SSLB) (Figure 5E). By day 25, most nephron structures resembled SSLBs (53.7%) followed by CSLBs (23.1%), RVs (12.1%) then PTAs (15.2%) (Figure 5E and G). Interestingly, Ang II shifted the distribution toward nephron maturation evidenced by an increased percentage of SSLBs (40.4 vs 69.5%; $P = .0007$) and fewer RVs (18.3 vs 7.0%; $P = 0.03$) per field of view. In contrast, losartan seemed to stall maturation, with a trend toward more PTAs (14.7 vs 22.0%; $P > .05$) and fewer RV (18.3 vs 11.6%; $P > .05$) (Figure 5E and G). On day 25, Ang II organoids had larger glomeruli (43.9 vs 70.7 µm; $P < .0001$), while losartan organoids had smaller glomeruli (43.9 vs 36.8 µm; $P < .0001$, Figure 5F), similar to day 16 glomerular results (Figure 5D). Consistent with these results, kidney organoids derived from the 1481 and 005B iPSC lines confirmed the effect of Ang II in shifting the distribution toward nephron maturation. However, there were slight differences with the 1481 line having more CSLBs (34.9 vs 19.7%; $P = .03$) and fewer RVs (4.3 vs 17.4%; $P = .02$) (Supplementary Figure S5A and B), while there was a trend toward more SSLBs (40.5 vs 52.2%; $P > .05$) and fewer RVs (20.7 vs 14.3%; $P > .05$) per field of view for the 005B line (Supplementary Figure S5C and D). The observed differences may be attributed to the developmental maturity and intrinsic differentiation potential of the iPSC lines. Overall, our results support the finding that nephron development is regulated by AT_1R signaling in human kidney organoids.

Discussion

Our study investigated the role of AT_1R signaling in nephrogenesis using human kidney organoids. Using various single-cell techniques and RNAscope as a validation tool, we uncovered a role for AT_1R signaling preferentially along the podocyte lineage. We showed that Ang II accelerated nephron maturation by upregulating epithelialization programs and suppressing self-renewal markers within podocyte precursor cells. Losartan maintained the progenitor state at the expense of epithelialization by sustaining the expression of self-renewal markers. These results provide further rationale for incorporating RAS modulators to improve organoid maturation. Indeed, collecting duct and intercalated cell differentiation is enhanced by aldosterone.[49]

RAS is traditionally studied using animal models due to its complexity and multiorgan nature. Because of its involvement in many human pathologies, in vitro systems that faithfully approximate human RAS physiology are required before high-throughput drug screening assays can be harnessed to develop pharmacologic agents that target various cardiovascular diseases. Recent studies have begun to identify critical components of RAS in human kidney organoids. In 2021, kidney organoids were reported to generate renin that is enzymatically active and responsive to parathyroid hormone as observed in vivo.[38,50] Our single-cell data expands on this by showing that *REN*$^+$ cells in kidney organoids possess a transcriptional profile similar to renin-producing fetal juxtaglomerular cells. Despite these encouraging similarities with in vivo RAS, the entire enzymatic cascade from renin to angiotensinogen, angiotensin I, and angiotensin II has not been characterized in kidney organoids.

Based on mathematical modeling, the cessation of nephrogenesis was predicted to be determined by an extrinsic physiological trigger rather than a molecular clock intrinsic to NP cells.[51] Our findings raise the possibility that AT_1R agonism is the trigger that depletes the NP pool at birth. In sheep, renal *AGTR1* is lowest during the first 60 days of gestation, peaks in the last trimester, and then drops in postnatal life.[52] Human plasma renin activity and aldosterone concentrations are highest in the first months of life before declining to adult levels.[53] Peak RAS activity at birth may explain accelerated differentiation of NP cells, depletion of the progenitor pool, and cessation of nephrogenesis. Future studies can validate this relationship in vivo.

Previous studies have demonstrated the crucial role of Ang II signaling in kidney development.[19,54,55] Exposure to ARBs or ACE inhibitors in utero causes tubular dysgenesis with poor differentiation of tubules, retraction of glomerular tufts, and thickened arteriolar walls.[56-59] Newborn rats given losartan

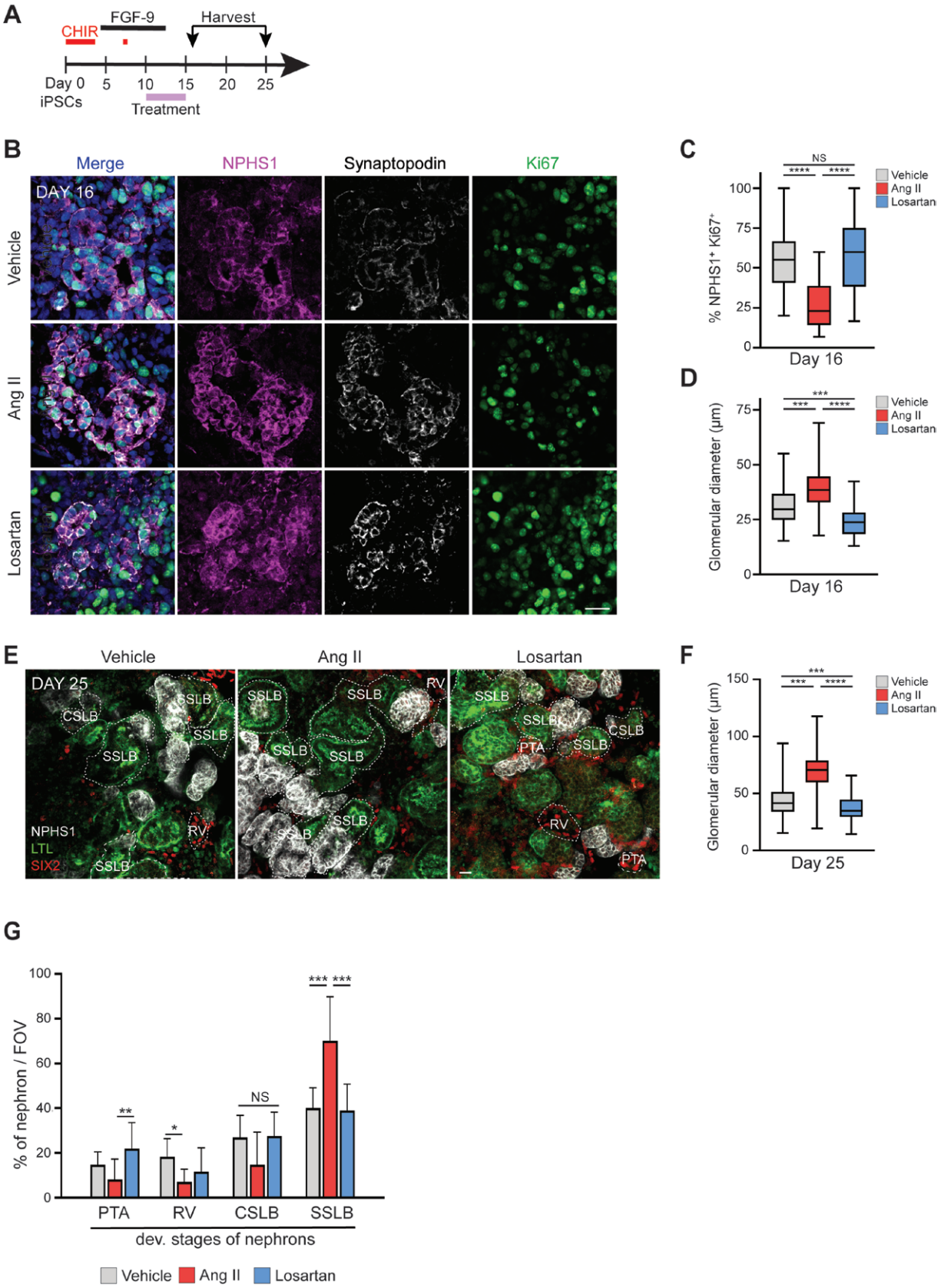

Figure 5. Nephron growth and maturation by AT_1R signaling. (A) Experimental plan for organoid treatment (purple bar) with Ang II and/or losartan. (B) Day 16 treated organoids immunostained with synaptopodin, NPHS1, and Ki67. Scale bar, 20 µm. (C-D) Quantification of glomerular diameter, and percent of proliferating NPHS1+ cells marked with Ki67 in day 16 organoids (n = 47-56) from 3 biological replicates using iPSC line CLi001-A. NS, not significant, Data are mean ± SD. ***P < .001, ****P < .0001. One-way ANOVA with post-hoc Tukey's multiple comparisons. (E) Morphological staging and quantification of developing nephrons (dashed lines) from day 25 organoids. Pre-tubular aggregates (PTA), renal vesicle (RV), comma-shaped like body (CSLB), and S-shaped like body (SSLB). Scale bar, 20 µ m. (F) Quantification of glomerular diameter in day 25 organoids (n = 76-101), representative of 3 biological replicates. Data are mean ± SD. ***P < .001 and ****P < .0001. One-way ANOVA with post-hoc Tukey's multiple comparisons. (G) Quantification of developing nephrons (dashed lines) from day 25 organoids of iPSC line CLi001-A. NS, not significant, Data are mean ± SD. *P < .05, **P < .01, ***P < 0.001. One-way ANOVA with post-hoc Tukey's multiple comparisons.

had significantly fewer glomeruli per kidney.[60] Glomerular growth was delayed in *AGTR1*-knockout mice.[61] In addition to the critical role of AT_1R signaling in glomerular development, our GO analysis supports an important contribution from AT_1R signaling for distal tubules and endothelial cell maturation (Supplementary Figure S3). Ang II upregulated pathways related to branching in ureteric bud morphogenesis, essential for the formation of renal collecting ducts,[62] the effects were downregulated by losartan. This finding is consistent with prior reports showing that Ang II stimulates ureteric bud cell proliferation in a dose-dependent manner, while AT_1R antagonist pretreatment inhibits the effect.[54,63] AT_1R signaling has been shown essential for blood vessel formation.[64,65] Our GO enrichment analysis revealed that Ang II upregulated pathways related to glomerular epithelial cell differentiation and distal tubule development, suggesting an indirect role for endothelial cells in nephron development (Supplementary Figure S3A). Similarly, losartan upregulated the pathways that impair vasculature development, further supporting the direct role of AT_1R in nephron development. These findings may help explain the clinical manifestations of tubular dysgenesis and arteriolar wall thickening, respectively.[59] It is possible that the cells expressing AT_1R and weakly expressing SIX2 may also indirectly modulate DTC and endothelial cells as these clusters neither expressed *AGTR1* nor *AGTR2* (Fig. 3A). Further studies are needed to validate our *in silico* findings in distal tubules and endothelial cells.

Our GO analyses and RNAscope data suggest that AT_1R agonism may coordinate the morphogenetics and patterning of the nephron during kidney development. Lineage tracing experiments would help evaluate AT_1R-mediated differentiation in the context of the gradual recruitment model. Alternatively, NP fate during AT_1R-mediated differentiation may vary as the organoid RAS matures. Indeed, *AGTR1* expression peaks by day 15 before decreasing and plateauing by day 22-25.[66] NP fate specification during AT_1R-mediated differentiation may be determined by the stoichiometry of RAS factors in developing organoids.

Our study has several limitations. First, the single-cell analysis was limited to one timepoint in organoid development. Second, losartan is a prodrug and requires metabolic modifications to generate the active metabolite. Different AT_1R blockers would be needed to validate our findings. Third, the optimal dose, duration, and combination of RAS modulators required to optimize nephron maturity in organoids was not addressed. Finally, the in vivo relevance and confirmation of AT_1R-mediated nephron fate specification requires further exploration. Future experiments using animal models are needed to validate the developmental role of RAS in nephrogenesis, progenitor exhaustion, and kidney lifespan.

Materials and methods

Ethical considerations

All experiments involving human biospecimens were approved by the Conjoint Health Research Ethics Board at the University of Calgary (REB20-1999). Informed consent was obtained from the healthy donor of peripheral blood mononuclear cells (PBMCs) for the generation of iPSC using an approved protocol according to a standardized procedure.

PBMC reprogramming

Peripheral blood mononuclear cells (PBMCs) from a healthy volunteer were isolated using Sepmate-15 tubes (Stem Cell Technologies, #15410) and cultured for 7 days in StemSpan SFEM II medium (Stem Cell Technologies, #09605) supplemented with erythroid expansion supplements (Stem Cell Technologies, #02692) to differentiate into CD34+ erythroid progenitor cells, following the manufacturer's instructions. A total of 1.0×10^6 CD34+ progenitor cells were nucleofected with episomal vectors from the Epi5 Episomal iPSC Reprogramming Kit (Thermo, A15960) using the Amaxa CD34 + kit (Lonza, #VPA-1003) and a Nucleofector 2b device (Lonza, U-014 program). The nucleofected cells were plated in 3 wells of a 6-well plate coated with Matrigel (Corning, #354277) and cultured in erythroid progenitor medium, gradually transitioning to ReproTeSR medium (Stem Cell Technologies, #05926) as per the manufacturer's protocol. iPSC colonies emerged within 14 days. A single healthy clone was manually selected, expanded, and cultured on Matrigel-coated plates in mTeSR medium (Stem Cell Technologies, #85850). This newly established line from the **C**hun **L**aboratory, **CL**i001-A, was confirmed to have no chromosomal abnormalities using G-band karyotyping and tested negative for Mycoplasma infection.

Culturing of iPSC

Human iPSC lines for this study were CLi001-A, 005B23.1 (referred to as 005B) was derived from skin punch fibroblast (gift from Dr. Li-Fang Chu; reprogrammed in the laboratory of Dr. James Thompson)[67,68] and 1481-G (referred to as 1481), human dermal fibroblast (Cell Applications, Inc. Cat. #106-05n, lot #1481 using CytoTune-iPS 2.0 Sendai reprogramming kit (Life Technologies Cat. #A16517) at the Harvard Stem Cell Institute iPS Core Facility was a gift from Dr. Martin Pollak.[69] iPSC were confirmed to be of normal karyotype and maintained with daily medium changes of mTeSR1 medium in 6 well plates coated with Matrigel®. Cells were passaged using GCDR and transferred to T25 flasks coated with Matrigel prior to differentiation. iPSC were routinely tested and confirmed negative for mycoplasma.

Generation of kidney organoids

Kidney organoids were differentiated using a protocol adapted from Takasato et al with minor modifications.[70] Modifications included APEL2 medium supplemented with 5% PFHM-II (APEL2 + PFHM) in replacement of APEL. Induced PSCs established in Matrigel matrix-coated T25 flask were treated with 8 µM CHIR99021 for 4 days followed by recombinant human FGF-9 (200 ng/mL) and heparin (1 µg/mL) for an additional 3 days. On day 7, cells were dissociated into single cells using trypsin for 2 min 500K cells were pelleted at 400 x *g* for 2 min and 4 pellets were transferred onto a 6-well transwell plate (Corning Cat. # 07-200-170). Pellets were incubated with a pulse of 5 µM CHIR99021 in APEL2 + PFHM medium for 1 h at 37°C, 5% CO_2. After 1 hour, the medium was changed to APEL2 + PFHM supplemented with FGF-9 (200 ng/mL) and heparin (1 µg/mL) for an additional 6 days. Kidney organoids were maintained in APEL2 + PFHM medium for 14 days with medium change every other day.

Treatment with RAS modulators

Kidney organoids were treated with Ang II (1 µM, Millipore Sigma, Cat. #A9525) or losartan (100 µM, Tocris, Cat.

#3798) in APEL2 + PFHM medium from days 10 to 15 or days 27-28. The Ang II or losartan treatment was replenished every other day. DMSO was used as a vehicle control. When co-treated, organoids were first pre-treated with losartan for 30 minutes before the addition of Ang II.

Wholemount immunofluorescence

Kidney organoids treated with Ang II and/or losartan were washed in PBS and fixed with 2% paraformaldehyde for 20 minutes at 4°C. Then, organoids were washed in PBS twice and blocked in blocking buffer containing 10% donkey serum, and 0.05% Triton-X in PBS for 2-3 hours at room temperature. Primary antibodies to NPHS1 (R&D Systems, Cat. #AF4269), PDGFR-β (Cell Signaling, Cat. #4564), E-Cadherin (BD Transduction laboratories, Cat. #610181), Synaptopodin (SCBT, Cat. #sc-515842), SIX2 (ProteinTech, Cat. #11562-1-AP), CD31 (BD Pharmingen, 555444), and AT1R (ThermoFisher, Cat. #MA5-42535). After 6 washes with wash buffer (0.3% Triton X-100 in PBS) for 10 minutes each wash, organoids were incubated with fluorescent conjugated secondary antibodies (Alexa Fluor donkey anti-mouse 405 (ThermoFisher), donkey anti-rabbit 568 (Invitrogen), donkey anti-sheep 647 (Invitrogen), donkey anti-mouse 647 (Invitrogen) or LTL-FITC (Vector laboratories, Cat. #FL-1321-2) for 2 hours at room temperature. After 3 washes with PBS, the samples were mounted onto slide with ProLong glass antifade mountant. Confocal images were acquired with Zeiss LSM 880 and Leica SP8 spectral confocal microscope using at least 3 technical replicates from each set of organoids.

RNAscope-IHC

In situ hybridization was performed on paraffin-embedded kidney organoids using RNAscope probes and the Multiplex Fluorescent V2 assay kit (ACD, #323100), following the manufacturer's instructions. Organoid sections (3 µm) were deparaffinized, rehydrated with ethanol, and treated with peroxidase. Antigen retrieval was performed in a steamer for 15 minutes. RNAscope probes or a negative control probe targeting DapB (ACD, #310043) were hybridized to the sections at 40°C for 2 hours in a HybEZ oven (ACD). The following probes were used in this study: Hs-SIX1 (ACD, 412401); Hs-OLFM3-C2 (ACD, 549051-C2); Hs-NPHS2-C3 (ACD, 556531-C3). Opal fluorophores (Opal 520, 570, and 650; Akoya Biosciences) were incubated for 30 minutes. A standard immunofluorescence staining was performed to label podocytes using an anti-NPHS1 antibody (R&D Systems, #AF4269). Sections were mounted with Prolong Gold Antifade mounting medium. For RNAscope quantification, the number of *SIX1*, *NPHS2,* or *OLFM3* positive pixels within NPHS1 + glomeruli were quantified and normalized to the total area of the glomerulus.

Analysis of differentially expressed genes and gene ontology enrichment analysis

Details for the scRNA-seq library construction and analysis of differentially expressed genes (DEG) are available in our previous study.[29] DEG from subclusters treated with Ang II or losartan were identified by calculating the fold change between each class's average feature expression, requiring a minimum of 20% expression. For our gene ontology (GO) enrichment analysis, we used The Gene Ontology Consortium's online tool (http://www.geneontology.org/) for the enrichment analysis of our gene lists. Genes were selected for GO analysis if their expression showed a fold change of >1.2 or <0.8 relative to controls. GO analyses for biological process pathways were conducted using the Panther v19.0 online tool (pantherdb.org), with statistical significance assessed via Fisher's exact test.[71,72] Enriched GO terms were ranked based on fold enrichment, and only results with a false discovery rate (FDR) of P-value < .05 were considered significant.

Organoid connectivity and cluster-specific perturbation

To interrogate cell-to-cell connectivity across the 5 main kidney cell types identified in Figure 1, we employed Connectome R toolkit v0.2.2 developed by Niklason Lab[42] using default and recommended parameters. Briefly, CreateConnectome function was used to query Seurat v3 object housing kidney organoid transcriptomes to define baseline nodes and edges for network analysis. Edges were filtered to only include receptor-ligand pairs with z-score above 0.3 and expression detected in at least 20% of cells in their respective clusters. To perform pairwise treatment comparisons, two comparators were provided to the DifferentialConnectome function, and output edges were filtered for P-adjusted < .05. CircosPlot and CircosDiff functions (wrappers around the R package circlize) were used to visualize cell-cell connectivity. Cluster-specific perturbations in response to treatment were quantified as $\sum \log_2$[fold change from control]. Calculated scores were visualized as hexbin plots using the Schex package with 40 bins partitioning the range of perturbation scores.

Trajectory inference during organoid maturation

NP trajectory inferences were performed by reprocessing reads in CellRanger BAMs with RNA velocity's *run10x* function using GRCh38 annotations as described previously.[73,74] Briefly, output looms were combined to examine the effects of angiotensin II, losartan, and their combination on tubular and podocyte differentiation. Merged looms were imported into Seurat (v. 4-5) using *ReadVelocity* found in *SeuratWrappers* (v.0.2.0), normalized using *SCTransform* (v. 0.3.2),[75,76] and exported in H5 format using *SaveH5Seurat* and *Convert* functions. Counts stored in H5 files were imported, filtered, and normalized as recommended by *scVelo* (v. 0.2.1) pipeline.[44] RNA velocity estimates were derived using stochastic and dynamical models. Given both models produced comparable outcomes, the stochastic model was selected as the standard method for all further analyses. Treatment-specific top-likelihood genes were calculated using *tl.rank_dynamical_genes* which ranks genes by their likelihood using the dynamical model. Podocyte and tubular states were annotated by plotting spliced levels of state-specific markers. Vector field topology was learned in the PCA space with Dynamo.[47] This enabled *in silico* perturbation predictions of renal cell fates using *dyn.pd.perturbation* function. This was employed to either activate or suppress gene activity, enabling visualization of how perturbations impact developmental trajectories.

Assessing podocyte maturation using human fetal kidney reference

We trained a machine learning classifier using scPred[48] to distinguish podocytes at fetal weeks 15 and 17. The classifier was based on scRNAseq of fetal human kidneys (GSE124472).[34] We merged zones 1 and 2 by a fetal week of development for this analysis. Our approach to feature selection for building this classifier was like our previous work focusing on the top

50 principal components (PCs) that each accounted for a minimum of 0.01% of the variance.[76] We trained using *trainModel* function, employing Support Vector Machines with a Radial Basis Function Kernel (model = *svmRadial*). A trained classifier was applied to nephron progenitors and the podocyte lineage from control and treated organoids. Proportions of scPred-inferred states were plotted using ggplot2 (v.3.1.1).

Quantification and Statistical Analysis

All statistical analyses and graphical representations were performed using Microsoft Excel v16, GraphPad Prism 9.4, and R version 3.6.3. The significance between 2 parametric groups was determined using Student's *t*-test. Significance between 2 non-parametric groups was determined using Wilcoxon signed-rank test. For comparisons between multiple groups, One-way ANOVA with post-hoc Tukey's multiple comparisons were employed. The significance between categorical data was determined using chi-squared test. For all tests, significance was defined as P value < .05.

Acknowledgments

Support for infrastructure and technical assistance was provided by the Live Cell Imaging Facility and the Human Organoid Innovation Hub at the Snyder Institute for Chronic Diseases, University of Calgary. Graphical abstract created with the aid of Biorender (https://www.biorender.com/).

Author contributions

WR and JC wrote the manuscript and drafted the figures. HC and SS co-wrote the manuscript. WR, AI, HC and JC cultured and treated the kidney organoids. WR, HC and AI stained and imaged the organoids. HC and AI performed RNAscope and quantification. SS and JB sequenced the organoids. SS, WR and AP analyzed the scRNAseq dataset. SS, RA and AJ designed and developed the Kidney Organoid Atlas. JC and WR conceived the experiments. JC supervised the study with JB.

Conflicts of interest

The authors have no competing interests to declare.

Funding

This work was supported by a new investigator award to JC from the Kidney Research Scientist Core Education and National Training Program.

Data Availability

Single cell RNA-Seq data are available at NCBI GEO with the following accession number: GSE149687.

Supplementary material

Supplementary material is available at *Stem Cells* online.

References

1. Luyckx VA, Rule AD, Tuttle KR, et al. Nephron overload as a therapeutic target to maximize kidney lifespan. *Nat Rev Nephrol.* 2022;18:171-183. https://doi.org/10.1038/s41581-021-00510-7
2. Kobayashi A, Valerius MT, Mugford JW, et al. Six2 defines and regulates a multipotent self-renewing nephron progenitor population throughout mammalian kidney development. *Cell Stem Cell.* 2008;3:169-181. https://doi.org/10.1016/j.stem.2008.05.020
3. Boyle S, Misfeldt A, Chandler KJ, et al. Fate mapping using Cited1-CreERT2 mice demonstrates that the cap mesenchyme contains self-renewing progenitor cells and gives rise exclusively to nephronic epithelia. *Dev Biol.* 2008;313:234-245. https://doi.org/10.1016/j.ydbio.2007.10.014
4. Schnell J, Achieng M, Lindstrom NO. Principles of human and mouse nephron development. *Nat Rev Nephrol.* 2022;18:628-642. https://doi.org/10.1038/s41581-022-00598-5
5. Park JS, Valerius MT, McMahon AP. Wnt/beta-catenin signaling regulates nephron induction during mouse kidney development. *Development.* 2007;134:2533-2539. https://doi.org/10.1242/dev.006155
6. Chung E, Deacon P, Marable S, Shin J, Park J-S. Notch signaling promotes nephrogenesis by downregulating Six2. *Development.* 2016;143:3907-3913. https://doi.org/10.1242/dev.143503
7. Narlis M, Grote D, Gaitan Y, Boualia SK, Bouchard M. Pax2 and pax8 regulate branching morphogenesis and nephron differentiation in the developing kidney. *J Am Soc Nephrol.* 2007;18:1121-1129. https://doi.org/10.1681/ASN.2006070739
8. Dudley AT, Lyons KM, Robertson EJ. A requirement for bone morphogenetic protein-7 during development of the mammalian kidney and eye. *Genes Dev.* 1995;9:2795-2807. https://doi.org/10.1101/gad.9.22.2795
9. Grieshammer U, Cebrián C, Ilagan R, et al. FGF8 is required for cell survival at distinct stages of nephrogenesis and for regulation of gene expression in nascent nephrons. *Development.* 2005;132:3847-3857. https://doi.org/10.1242/dev.01944
10. Basta JM, Robbins L, Kiefer SM, Dorsett D, Rauchman M. Sall1 balances self-renewal and differentiation of renal progenitor cells. *Development.* 2014;141:1047-1058. https://doi.org/10.1242/dev.095851
11. Xu J, Wong EYM, Cheng C, et al. Eya1 interacts with Six2 and Myc to regulate expansion of the nephron progenitor pool during nephrogenesis. *Dev Cell.* 2014;31:434-447. https://doi.org/10.1016/j.devcel.2014.10.015
12. Perl AJ, Schuh MP, Kopan R. Regulation of nephron progenitor cell lifespan and nephron endowment. *Nat Rev Nephrol.* 2022;18:683-695. https://doi.org/10.1038/s41581-022-00620-w
13. Kispert A, Vainio S, McMahon AP. Wnt-4 is a mesenchymal signal for epithelial transformation of metanephric mesenchyme in the developing kidney. *Development.* 1998;125:4225-4234. https://doi.org/10.1242/dev.125.21.4225
14. Stark K, Vainio S, Vassileva G, McMahon AP. Epithelial transformation of metanephric mesenchyme in the developing kidney regulated by Wnt-4. *Nature.* 1994;372:679-683. https://doi.org/10.1038/372679a0
15. Lawlor KT, Zappia L, Lefevre J, et al. Nephron progenitor commitment is a stochastic process influenced by cell migration. *Elife.* 2019;8:e41156. https://doi.org/10.7554/eLife.41156
16. Short KM, Combes AN, Lefevre J, et al. Global quantification of tissue dynamics in the developing mouse kidney. *Dev Cell.* 2014;29:188-202. https://doi.org/10.1016/j.devcel.2014.02.017
17. Chen S, Brunskill EW, Potter SS, et al. Intrinsic age-dependent changes and cell-cell contacts regulate nephron progenitor lifespan. *Dev Cell.* 2015;35:49-62. https://doi.org/10.1016/j.devcel.2015.09.009
18. Jarmas AE, Brunskill EW, Chaturvedi P, Salomonis N, Kopan R. Progenitor translatome changes coordinated by Tsc1 increase perception of Wnt signals to end nephrogenesis. *Nat Commun.* 2021;12:6332. https://doi.org/10.1038/s41467-021-26626-9
19. Yosypiv IV. Renin-angiotensin system in mammalian kidney development. *Pediatr Nephrol.* 2021;36:479-489. https://doi.org/10.1007/s00467-020-04496-5
20. Schutz S, Le Moullec JM, Corvol P, Gasc JM. Early expression of all the components of the renin-angiotensin-system in human development. *Am J Pathol.* 1996;149:2067-2079.

21. Gribouval O, Gonzales M, Neuhaus T, et al. Mutations in genes in the renin-angiotensin system are associated with autosomal recessive renal tubular dysgenesis. *Nat Genet*. 2005;37:964-968. https://doi.org/10.1038/ng1623
22. Lacoste M, Cai Y, Guicharnaud L, et al. Renal tubular dysgenesis, a not uncommon autosomal recessive disorder leading to oligohydramnios: role of the Renin-Angiotensin system. *J Am Soc Nephrol*. 2006;17:2253-2263. https://doi.org/10.1681/ASN.2005121303
23. Nadeem S, Hashmat S, Defreitas MJ, et al. Renin angiotensin system blocker fetopathy: a Midwest Pediatric Nephrology Consortium Report. *J Pediatr*. 2015;167:881-885. https://doi.org/10.1016/j.jpeds.2015.05.045
24. Weber-Schoendorfer C, Kayser A, Tissen-Diabaté T, et al. Fetotoxic risk of AT1 blockers exceeds that of angiotensin-converting enzyme inhibitors: an observational study. *J Hypertens*. 2020;38:133-141. https://doi.org/10.1097/HJH.0000000000002233
25. Song R, Kidd L, Janssen A, Yosypiv IV. Conditional ablation of the prorenin receptor in nephron progenitor cells results in developmental programming of hypertension. *Physiol Rep*. 2018;6:e13644. https://doi.org/10.14814/phy2.13644
26. Waehle V, Ungricht R, Hoppe PS, Betschinger J. The tumor suppressor WT1 drives progenitor cell progression and epithelialization to prevent Wilms tumorigenesis in human kidney organoids. *Stem Cell Rep*. 2021;16:2107-2117. https://doi.org/10.1016/j.stemcr.2021.07.023
27. Tanigawa S, Islam M, Sharmin S, et al. Organoids from nephrotic disease-derived iPSCs identify impaired NEPHRIN localization and slit diaphragm formation in kidney podocytes. *Stem Cell Rep*. 2018;11:727-740. https://doi.org/10.1016/j.stemcr.2018.08.003
28. Freedman BS, Brooks CR, Lam AQ, et al. Modelling kidney disease with CRISPR-mutant kidney organoids derived from human pluripotent epiblast spheroids. *Nat Commun*. 2015;6:8715. https://doi.org/10.1038/ncomms9715
29. Rahmani W, Chung H, Sinha S, et al. Attenuation of SARS-CoV-2 infection by losartan in human kidney organoids. *iScience*. 2022;25:103818. https://doi.org/10.1016/j.isci.2022.103818
30. Chung H, Bui-Marinos MP, Rahmani W, Corcoran JA, Chun J. Infecting kidney organoids with a cDNA reporter clone of SARS-CoV-2. *STAR Protoc*. 2022;3:101617. https://doi.org/10.1016/j.xpro.2022.101617
31. Takasato M, Er PX, Chiu HS, et al. Kidney organoids from human iPS cells contain multiple lineages and model human nephrogenesis. *Nature*. 2015;526:564-568. https://doi.org/10.1038/nature15695
32. Lindstrom NO, McMahon JA, Guo J, et al. Conserved and divergent features of human and mouse kidney organogenesis. *J Am Soc Nephrol*. 2018;29:785-805. https://doi.org/10.1681/ASN.2017080887
33. Combes AN, Zappia L, Er PX, Oshlack A, Little MH. Single-cell analysis reveals congruence between kidney organoids and human fetal kidney. *Genome Med*. 2019;11:3. https://doi.org/10.1186/s13073-019-0615-0
34. Tran T, Lindström NO, Ransick A, et al. In vivo developmental trajectories of human podocyte inform in vitro differentiation of pluripotent stem cell-derived podocytes. *Dev Cell*. 2019;50:102-116.e6. https://doi.org/10.1016/j.devcel.2019.06.001
35. Phipson B, Er PX, Combes AN, et al. Evaluation of variability in human kidney organoids. *Nat Methods*. 2019;16:79-87. https://doi.org/10.1038/s41592-018-0253-2
36. Wu H, Uchimura K, Donnelly EL, et al. Comparative analysis and refinement of human PSC-derived kidney organoid differentiation with single-cell transcriptomics. *Cell Stem Cell*. 2018;23:869-881.e8. https://doi.org/10.1016/j.stem.2018.10.010
37. Brunskill EW, Sequeira-Lopez MLS, Pentz ES, et al. Genes that confer the identity of the renin cell. *J Am Soc Nephrol*. 2011;22:2213-2225. https://doi.org/10.1681/ASN.2011040401
38. Shankar AS, Du Z, Mora HT, et al. Human kidney organoids produce functional renin. *Kidney Int*. 2021;99:134-147. https://doi.org/10.1016/j.kint.2020.08.008
39. Motojima M, Tanaka M, Kume T. Foxc1 and Foxc2 are indispensable for the maintenance of nephron and stromal progenitors in the developing kidney. *J Cell Sci*. 2022;135:jcs260356. https://doi.org/10.1242/jcs.260356
40. Self M, Lagutin OV, Bowling B, et al. Six2 is required for suppression of nephrogenesis and progenitor renewal in the developing kidney. *EMBO J*. 2006;25:5214-5228. https://doi.org/10.1038/sj.emboj.7601381
41. Levinson R, Mendelsohn C. Stromal progenitors are important for patterning epithelial and mesenchymal cell types in the embryonic kidney. *Semin Cell Dev Biol*. 2003;14:225-231. https://doi.org/10.1016/s1084-9521(03)00025-9
42. Raredon MSB, Adams TS, Suhail Y, et al. Single-cell connectomic analysis of adult mammalian lungs. *Sci Adv*. 2019;5:eaaw3851. https://doi.org/10.1126/sciadv.aaw3851
43. Howden SE, Vanslambrouck JM, Wilson SB, Tan KS, Little MH. Reporter-based fate mapping in human kidney organoids confirms nephron lineage relationships and reveals synchronous nephron formation. *EMBO Rep*. 2019;20:e47483. https://doi.org/10.15252/embr.201847483
44. Bergen V, Lange M, Peidli S, Wolf FA, Theis FJ. Generalizing RNA velocity to transient cell states through dynamical modeling. *Nat Biotechnol*. 2020;38:1408-1414. https://doi.org/10.1038/s41587-020-0591-3
45. Edwards JC. What's a CLIC doing in the podocyte? *Kidney Int*. 2010;78:831-833. https://doi.org/10.1038/ki.2010.238
46. Ashraf S, Kudo H, Rao J, et al. Mutations in six nephrosis genes delineate a pathogenic pathway amenable to treatment. *Nat Commun*. 2018;9:1960. https://doi.org/10.1038/s41467-018-04193-w
47. Qiu X, Zhang Y, Martin-Rufino JD, et al. Mapping transcriptomic vector fields of single cells. *Cell*. 2022;185:690-711.e45. https://doi.org/10.1016/j.cell.2021.12.045
48. Alquicira-Hernandez J, Sathe A, Ji HP, Nguyen Q, Powell JE. scPred: accurate supervised method for cell-type classification from single-cell RNA-seq data. *Genome Biol*. 2019;20:264. https://doi.org/10.1186/s13059-019-1862-5
49. Uchimura K, Wu H, Yoshimura Y, Humphreys BD. Human pluripotent stem cell-derived kidney organoids with improved collecting duct maturation and injury modeling. *Cell Rep*. 2020;33:108514. https://doi.org/10.1016/j.celrep.2020.108514
50. Broulik PD, Horky K, Pacovsky V. Effect of parathyroid hormone on plasma renin activity in humans. *Horm Metab Res*. 1986;18:490-492. https://doi.org/10.1055/s-2007-1012353
51. Zubkov VS, Combes AN, Short KM, et al. A spatially-averaged mathematical model of kidney branching morphogenesis. *J Theor Biol*. 2015;379:24-37. https://doi.org/10.1016/j.jtbi.2015.04.015
52. Robillard JE, Page WV, Mathews MS, et al. Differential gene expression and regulation of renal angiotensin II receptor subtypes (AT1 and AT2) during fetal life in sheep. *Pediatr Res*. 1995;38:896-904. https://doi.org/10.1203/00006450-199512000-00012
53. Dillon MJ, Ryness JM. Plasma renin activity and aldosterone concentration in children. *Br Med J*. 1975;4:316-319. https://doi.org/10.1136/bmj.4.5992.316
54. Yosypiv IV, El-Dahr SS. Role of the renin-angiotensin system in the development of the ureteric bud and renal collecting system. *Pediatr Nephrol*. 2005;20:1219-1229. https://doi.org/10.1007/s00467-005-1944-3
55. Wolf G. Angiotensin II and tubular development. *Nephrol Dial Transplant*. 2002;17:48-51. https://doi.org/10.1093/ndt/17.suppl_9.48
56. Cox RM, Anderson JM, Cox P. Defective embryogenesis with angiotensin II receptor antagonists in pregnancy. *BJOG*. 2003;110:1038.
57. Saji H, Yamanaka M, Hagiwara A, Ijiri R. Losartan and fetal toxic effects. *Lancet*. 2001;357:363. https://doi.org/10.1016/S0140-6736(00)03648-5
58. Lambot MA, Vermeylen D, Noel JC. Angiotensin-II-receptor inhibitors in pregnancy. *Lancet*. 2001;357:1619-1620. https://doi.org/10.1016/s0140-6736(00)04757-7

59. Martinovic J, Benachi A, Laurent N, Daikha-Dahmane F, Gubler MC. Fetal toxic effects and angiotensin-II-receptor antagonists. *Lancet*. 2001;358:241-242. https://doi.org/10.1016/S0140-6736(01)05426-5
60. Woods LL, Rasch R. Perinatal ANG II programs adult blood pressure, glomerular number, and renal function in rats. *Am J Physiol*. 1998;275:R1593-R1599. https://doi.org/10.1152/ajpregu.1998.275.5.R1593
61. Tsuchida S, Matsusaka T, Chen X, et al. Murine double nullizygotes of the angiotensin type 1A and 1B receptor genes duplicate severe abnormal phenotypes of angiotensinogen nullizygotes. *J Clin Invest*. 1998;101:755-760. https://doi.org/10.1172/JCI1899
62. Costantini F, Kopan R. Patterning a complex organ: branching morphogenesis and nephron segmentation in kidney development. *Dev Cell*. 2010;18:698-712. https://doi.org/10.1016/j.devcel.2010.04.008
63. Iosipiv IV, Schroeder M. A role for angiotensin II AT1 receptors in ureteric bud cell branching. *Am J Physiol Renal Physiol*. 2003;285:F199-F207. https://doi.org/10.1152/ajprenal.00401.2002
64. Madsen K, Marcussen N, Pedersen M, et al. Angiotensin II promotes development of the renal microcirculation through AT1 receptors. *J Am Soc Nephrol*. 2010;21:448-459. https://doi.org/10.1681/ASN.2009010045
65. Tufro-McReddie A, Romano LM, Harris JM, Ferder L, Gomez RA. Angiotensin II regulates nephrogenesis and renal vascular development. *Am J Physiol*. 1995;269:F110-F115. https://doi.org/10.1152/ajprenal.1995.269.1.F110
66. Yanofsky SM, Dugas CM, Katsurada A, et al. Angiotensin II biphasically regulates cell differentiation in human iPSC-derived kidney organoids. *Am J Physiol Renal Physiol*. 2021;321:F559-F571. https://doi.org/10.1152/ajprenal.00134.2021
67. Hou Z, Zhang Y, Propson NE, et al. Efficient genome engineering in human pluripotent stem cells using Cas9 from Neisseria meningitidis. *Proc Natl Acad Sci U S A*. 2013;110:15644-15649. https://doi.org/10.1073/pnas.1313587110
68. Zhang J, Chu L-F, Hou Z, et al. Functional characterization of human pluripotent stem cell-derived arterial endothelial cells. *Proc Natl Acad Sci U S A*. 2017;114:E6072-E6078. https://doi.org/10.1073/pnas.1702295114
69. Chun J, Riella CV, Chung H, et al. DGAT2 inhibition potentiates lipid droplet formation to reduce cytotoxicity in APOL1 kidney risk variants. *J Am Soc Nephrol*. 2022;33:889-907. https://doi.org/10.1681/ASN.2021050723
70. Takasato M, Er PX, Chiu HS, et al. Kidney organoids from human iPS cells contain multiple lineages and model human nephrogenesis. *Nature*. 2016;536:238. https://doi.org/10.1038/nature17982
71. Ashburner M, Ball CA, Blake JA, et al. Gene ontology: tool for the unification of biology. The Gene Ontology Consortium. *Nat Genet*. 2000;25:25-29. https://doi.org/10.1038/75556
72. Aleksander SA, Balhoff J, Carbon S, et al; Gene Ontology Consortium. The Gene Ontology knowledgebase in 2023. *Genetics*. 2023;224:iyad031. https://doi.org/10.1093/genetics/iyad031
73. La Manno G, Soldatov R, Zeisel A, et al. RNA velocity of single cells. *Nature*. 2018;560:494-498. https://doi.org/10.1038/s41586-018-0414-6
74. Sinha S, Rosin NL, Arora R, et al. Dexamethasone modulates immature neutrophils and interferon programming in severe COVID-19. *Nat Med*. 2022;28:201-211. https://doi.org/10.1038/s41591-021-01576-3
75. Hafemeister C, Satija R. Normalization and variance stabilization of single-cell RNA-seq data using regularized negative binomial regression. *Genome Biol*. 2019;20:296. https://doi.org/10.1186/s13059-019-1874-1
76. Sinha S, Sparks HD, Labit E, et al. Fibroblast inflammatory priming determines regenerative versus fibrotic skin repair in reindeer. *Cell*. 2022;185:4717-4736.e25. https://doi.org/10.1016/j.cell.2022.11.004